



International Journal of Environment and Waste Management

ISSN online: 1478-9868 - ISSN print: 1478-9876
<https://www.inderscience.com/ijewm>

Removal of mineral scaling precursors from electro dialysis concentrate by alkaline precipitation

Emily Mayer Andrade Becheleni, Edward Michael Peters, Ricardo Perobelli Borba, Sônia Denise Ferreira Rocha

DOI: [10.1504/IJEW.2022.10033394](https://doi.org/10.1504/IJEW.2022.10033394)

Article History:

Received: 23 January 2020
Accepted: 12 July 2020
Published online: 22 March 2023

Removal of mineral scaling precursors from electro dialysis concentrate by alkaline precipitation

Emily Mayer Andrade Becheleni*

Institute of Engineering, Science and Technology,
Universidade Federal dos Vales do Jequitinhonha e Mucuri,
Avenida Um, 4.050 – Cidade Universitária,
Janaúba – Minas Gerais, 39447-814, Brazil
Email: emily.becheleni@ufvjm.edu.br

*Corresponding author

Edward Michael Peters

Chemical Engineering Department,
KTH Royal Institute of Technology,
SE-100 44, Stockholm, Sweden
Email: edwpet@kth.se

Ricardo Perobelli Borba

Geology and Natural Resource Department,
Universidade Estadual de Campinas,
Rua João Pandiá Calógeras, 51. Campinas,
São Paulo, 13083-870, Brazil
Email: borba@ige.unicamp.br

Sônia Denise Ferreira Rocha

Department of Mining Engineering,
Universidade Federal de Minas Gerais,
Avenida Antônio Carlos, 6627, Pampulha,
Belo Horizonte – Minas Gerais, 31270-901, Brazil
Email: sdrocha@demin.ufmg.br

Abstract: Evaporative crystallisation has been used to recover water for industrial reuse but it presents serious problems related to incrustation. In this perspective, alkaline precipitation is studied in the present work, aiming to remove scale-forming salts prior to evaporative crystallisation of a reverse electro dialysis concentrate (EDC). The concentration of inorganic species in the feed and filtrate streams were determined by ICP-OES. The total organic carbon and inorganic carbon were analysed by thermo-catalytic oxidation with high temperature to assess the removal of organic compounds from EDC. The software PHREEQC was used to model the systems and a comparison with experimental results confirmed the credibility of the experiments. The

technique proved to be a favourable method for removal of almost 100% of Ca and Mg by adding 0.04 wt.% of caustic soda. Furthermore, this would improve the downstream evaporative crystallisation efficiency due to reduced incrustation potential.

Keywords: PHREEQC; desalination; calcium carbonate; magnesium hydroxide; reverse electrodialysis; scaling; hydrogeochemical model; precipitation; water reuse; demineralisation process.

Reference to this paper should be made as follows: Becheleni, E.M.A., Peters, E.M., Borba, R.P. and Rocha, S.D.F. (2023) 'Removal of mineral scaling precursors from electrodialysis concentrate by alkaline precipitation', *Int. J. Environment and Waste Management*, Vol. 31, No. 1, pp.19–41.

Biographical notes: Emily Mayer Andrade Becheleni is a Professor at the Universidade Federal dos Vales do Jequitinhonha e Mucuri. She received her PhD from the Federal University of Minas Gerais (UFMG, Brazil) following research in crystallisation applied to wastewater treatment with focus on water recovery. Part of her PhD research was conducted at the University of Cape Town (UCT, South Africa). She then pursued post-doctoral research on leaching of laterite ore at the UFMG. Prior to her doctoral studies, she received her Master's degree in Mineral Engineering (flotation) and a Bachelor's degree in Industrial Chemistry from Federal University of Ouro Preto. Her research interests include mineral processing, separations processes, water and waste treatments and environmental issues.

Edward Michael Peters is graduated with a BEng (Hons) Chemical Engineering degree obtained from the National University of Science and Technology, Zimbabwe, and an MSc Chemical Engineering degree obtained from the University of Cape Town, South Africa. His main research areas include wastewater treatment, resource recovery and crystallisation. He pursued Master's degree research with focus on the effect of anti-scalants on the thermodynamics and crystallisation kinetics of sodium sulphate decahydrate from acid mine drainage. Currently, he is pursuing his PhD at KTH Royal Institute of Technology, Sweden, with focus on recovery of scandium from solvent extraction strip liquors using crystallisation techniques as part of the broader project on valorisation of scandium-bearing waste material such as bauxite residue. Other research interests include separation processes such as absorption, distillation, solvent extraction, leaching, adsorption and ion exchange.

Ricardo Perobelli Borba holds a degree in Geological Engineering from the Federal University of Ouro Preto (1993), Master's and PhD degrees from Geosciences at the State University of Campinas. Currently, he is a Professor at the Institute of Geosciences of the State University of Campinas. He has experience in geosciences, with emphasis in environmental geochemistry (soils, waters and sediments) and hydrogeochemical modelling (PHREEQC).

Sônia Denise Ferreira Rocha is a Full Professor in the Department of Mining Engineering at the Federal University of Minas Gerais (UFMG, Brazil) and CNPq Fellow Researcher. She obtained her Bachelor's degree in Chemical Engineering (1987), MSc (1991) and Doctor (1997) in Mining and Metallurgical Engineering from UFMG. She was a visiting scholar at HydroMET-Hydrothermal Materials for Environmental and Energy Technologies Laboratory – McGill University (2009–2010). She has experience in leaching, crystallisation, adsorption and aqueous mineral/metal processing with focus on high environmental performance.

1 Introduction

Reverse osmosis (RO) and reverse electro dialysis are well-known techniques used for desalination of brines and recovering water for industrial reuse (Zaviska et al., 2015; Mutamim et al., 2012; Kim, 2011; Mezher et al., 2011; Greenlee et al., 2009). Although these techniques recover potable water, they generate saline waste streams, which are disposed of in evaporative ponds since further treatment using desalination processes is limited by the increased scaling potential of the salts. Moreover, the ponds require vast areas of land, which become a limiting factor with time and may lead to environmental pollution. Crystallisation has been pointed out for further treatment of the concentrated brine streams to recover pure water and salts (Becheleni et al., 2014; Morillo et al., 2014; Macedonio et al., 2011; Reddy et al., 2010; Lewis et al., 2010).

Becheleni et al. (2014) evaluated the effectiveness of evaporative crystallisation to treat a reverse electro dialysis concentrate containing 0.5% NaCl to obtain pure water that could be re-used in heat exchangers. However, a major challenge encountered in this process was the precipitation of calcium carbonate and calcium sulphate during crystallisation since they attained supersaturation easily due to their low solubilities, before NaCl precipitated. Therefore, this study attempts to remove scale-forming ions in a pre-treatment step prior to evaporative crystallisation to improve the efficiency of the process so as to recover NaCl as well (Becheleni et al., 2014). Incrustation occurs due to an increase in the concentration of scale-forming ions leading to supersaturation, which results in primary or heterogeneous nucleation and growth of solids on vessel and pipe walls (Chaussemier et al., 2015; Liu et al., 2011; Hoang et al., 2007; Hoang et al., 2004; Adams and Papangelakis, 2000; Sudmalis and Sheikholeslami, 2000). This has several undesirable effects, which include damage to equipment, fouling, reduction of the equipment durability, impact on process operability and increase in energy consumption as well as decrease in productivity. Typical scaling salts include sulphates of calcium, magnesium, barium and strontium and carbonate salts as well as silica.

A process that integrates RO, chemical demineralisation and crystallisation of the brines produced may be a technically viable solution to operate membrane desalination processes working at a high level of water recovery. Gabelich et al. (2007, 2011) evaluated the effective desalination of Colorado River water at a continuous pilot scale system. The two-stage process involved intermediate chemical demineralisation (ICD) of the concentrate stream from a primary reverse osmosis (PRO) process using 30% NaOH followed by a secondary reverse osmosis desalting stage. The NaOH dosage to the solid contact reactor (SCR) feed was systematically varied over the test period to achieve SCR effluent pH within the range of 9.2–11.3. The authors observed that the increase in Ca removal with increase in pH was consistent with the rise in CaCO_3 supersaturation in the SCR resulting in precipitation thereof. Above pH 10, the Ca removal, primarily as calcium carbonate, was in the range of 94–97%. In addition, the overall water recovery was enhanced from 85% to 95% without any scaling of the ions present in RO feed for an operational period of 550 hours. The authors observed that the process was highly dependent on pH, Ca concentration and total carbonate concentration in the effluent and that Ba and Sr removal efficiencies were strongly correlated with that of Ca. High removal efficiencies were generally encountered above pH of 10, attributed to increased co-precipitation (possible via inclusion in the crystal lattice or surface adsorption or precipitation as separate crystalline phases) of Ba and Sr with increasing CaCO_3 precipitation at elevated pH. At pH above 10, the removal efficiencies obtained for Ca,

Ba, Sr and SiO₂ were greater than 94%, 97%, 88% and 67%, respectively. The Mg removal (38–80%) was primarily through Mg(OH)₂ co-precipitation with CaCO₃ (Gabelich et al., 2007).

In a separate investigation, Subramani et al. (2012) compared innovative concentrate treatment methods such as electrocoagulation with chemical softening methods to remove scaling precursors from groundwater obtained from a mining site in Chile. The concentrate presented silica levels exceeding 90 mgL⁻¹ in addition to high concentrations of calcium (>400 mgL⁻¹), sulphate (>1,700 mgL⁻¹) and some toxic metals such as Al, Zn, Mn, Hg, Ni, Fe and others. In these chemical softening experiments, different doses (3,000–5,000 mgL⁻¹) of calcium hydroxide (lime) and 2,500–3,000 mgL⁻¹ of sodium carbonate (soda ash) were added to the primary reverse osmosis concentrate to enhance the precipitation of calcium carbonate. As reported by the authors, a soda ash dose of 5,000 mgL⁻¹ for lime softening and 3,000 mgL⁻¹ for sodium carbonate softening were required at a pH of approximately 11.0–11.4 to decrease the calcium concentration below 20 mgL⁻¹ and for high magnesium removal rates. At the optimum soda ash and lime softening dosages, calcium and magnesium concentrations were reduced to 15 mgL⁻¹ and below 1 mgL⁻¹, respectively. The lime softening process achieved a silica removal of 80% and the sodium hydroxide softening reached a silica removal of 85%. For the optimum chemical softening conditions, the clarified supernatant had a turbidity of less than 0.5 nephelometric turbidity unit (NTU) and total suspended solids of less than 10 mgL⁻¹ after 60 minutes of settling. The chemical consumption was higher for lime softening compared to sodium hydroxide softening, due to the introduction of additional calcium ions from lime (Subramani et al., 2012).

Qu et al. (2009) investigated the integration of accelerated precipitation softening (APS) with direct contact membrane distillation (DCMD) to establish a desalination process for the high recovery desalination of primary reverse osmosis (PRO) concentrate at a laboratory scale. The APS process involved pH adjustment with 1 molL⁻¹ of sodium hydroxide solution of concentration 40 mgL⁻¹. Calcite or quartz seeds (5gL⁻¹) were dispersed in the PRO concentrate (10 L) before the precipitation. The authors reported that the solution pH increased from 9.10 to 11.10 corresponding to an increase in the calcium removal efficiency from 38% to 86%, over a period of 30 minutes. In addition, a load of 5 gL⁻¹ calcite seeds resulted in calcite removal up to 91%. The PRO concentrate before and after APS revealed that, the calcium removal efficiency as CaCO₃ and CaSO₄ was about 92% for both salts, while those of magnesium, sulphate and silica were 4.4%, 1.1% and 1.6%, respectively (Qu et al., 2009).

As reported by numerous desalination researchers, carbonate salts can be precipitated as calcium and/or magnesium carbonates whose precipitation kinetics depend on the Ca, Mg and carbonate concentration, supersaturation and pH (Santos et al., 2017; Blue and Dove, 2015; Becheleni et al., 2014; Subramani et al., 2012; Gabelich et al., 2011; Gabelich et al., 2007; Pokrovsky, 1998). The supersaturation index (SI) is useful in determining whether supersaturation has been achieved with respect to a particular salt. It is calculated as a ratio of the free ionic activity product (IAP) and the thermodynamic solubility product of the crystal phase (K_{sp}) (Mullin, 2001; Sloeyink and Jenkins, 1980). Sometimes, the logarithm of this ratio is taken to be the saturation index. The IAP is computed from the free ion activities, which are products of the activity coefficient of each ion and its actual concentration in solution. The thermodynamic driving force for crystallisation is given by the Gibbs free energy change accompanying the process, which is correlated to SI, as proposed by Sloeyink and Jenkins (1980), shown in equation (1).

$$\Delta G = (-2.303RT)SI \quad (1)$$

where R is the ideal gas constant and T is the temperature. The equilibrium condition is achieved when $SI = 0$ (expressed as a logarithm), $IAP = K_{sp}$ and $\Delta G = 0$. A state of supersaturation occurs when $SI > 0$, $IAP > K_{sp}$ and $\Delta G < 0$ indicating that crystals may be formed in solution. In an undersaturated system where crystals are not formed, $SI < 0$, $IAP < K_{sp}$ and $\Delta G > 0$.

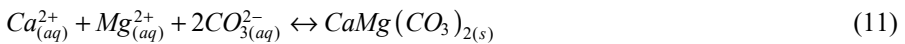
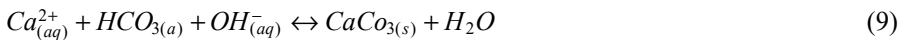
In this study, PHREEQC[®] was applied to the calculations of ion speciation and saturation index (SI) of different carbonates and magnesium hydroxide in chemically defined alkaline precipitation systems. The PHREEQC[®] software is a speciation program used to calculate saturation indices and the distribution of aqueous species whose mole balance can be defined for any valence state or combination of valence states for an element. A specified pH or any redox potential couple, for which data are available, is used as a basis for the distribution of redox elements among their valence states. The PHREEQC[®] software obtains a specified saturated index (or equilibrium) by adjusting the concentration of an element (specified with a variety of concentration units) for certain phase(s). This program uses ion-association and the Debye Hückel expressions to report the non-ideality of aqueous solutions, based on their activity coefficients. This type of aqueous model is valid at low ionic strength ($<0.1 \text{ mol kg}^{-1}$). For higher ionic strengths such as those typical of seawater, the model does not work. The ionic-strength term in the Debye Hückel expressions can be used to extend the range of applicability of the aqueous model (Truesdell and Jones, 1974). Therefore, in sodium chloride systems, as the case of reverse electro dialysis concentrate studied here, the model may be reliable at higher ionic strengths. For high ionic strength solutions, the specific interaction approach to thermodynamic properties of aqueous solutions should be used (Pitzer, 1979; Harvie and Weare, 1989).

The use of modelling software such as PHREEQC[®] (Parkhurst and Appelo, 2013) for predictions of the saturation indices of salts in aqueous systems based on thermodynamic data is extremely helpful, due to the many equilibrium possibilities in carbonate systems associated with scaling formation. This geochemical model is capable of simulating equilibrium reactions between minerals and water, ion exchangers, mineral dissolution and precipitation, surface complexation and other reactions (Parkhurst and Appelo, 2013; Betrie et al., 2016; Song et al., 2015; Charlton and Parkhurst, 2011; Rock et al., 2001).

The Gibbs free energies of formation (ΔG_f°) of $\text{CaCO}_{3(s)}$ and $\text{MgCO}_{3(s)}$ are $-1,125 \text{ kJ mol}^{-1}$ (Mullin, 2001) and $-1,007 \text{ kJ mol}^{-1}$ (Cheng et al., 2014), respectively. For dolomite, the theoretical ΔG_f° is $-2,147 \text{ kJ mol}^{-1}$ and the theoretical enthalpy of formation of dolomite from a 50:50 mixture of calcite and magnesite ($\text{Ca}_{0.5}\text{Mg}_{0.5}\text{CO}_{3(s)}$) calculated by Rock and co-authors was $-11.56 \pm 2.20 \text{ kJ mol}^{-1}$ at room temperatures ($25\text{--}28^\circ\text{C}$) and 1 atm (Cheng et al., 2014). These negative values for Gibb's free energy of formation are typical of spontaneous reactions, but the nuclei of those with lower activation energy are generated first (Sangwal, 2007). The Arrhenius activation energy for calcite precipitation is about 10 kcal mol^{-1} in the temperature range of $10\text{--}40^\circ\text{C}$ (Plummer et al., 1978; Nancollas and Reddy, 1971; Wiechers et al., 1975; Kazmierczak et al., 1982). For hydrothermal and sedimentary dolomite, the respective activation energies are in the ranges of $12.2\text{--}38 \text{ kcal mol}^{-1}$ and $7\text{--}13 \text{ kcal mol}^{-1}$, (Busenberg and Plummer, 1982) and for magnesite precipitation, this energy is about $15.8\text{--}21.2 \text{ kcal mol}^{-1}$.

¹ (Faux et al., 1986). For brucite, the Arrhenius activation energy is about 10 kcal mol⁻¹ (Pokrovsky and Schott, 2004; Vermilyea, 1969; Mejias et al., 1999).

The reactions between carbon dioxide and alkaline metals (Ca and Mg) in brines are widely known and represented by equations (2) to (11) (Sloevink and Jenkins, 1980; Sanjuan and Girard, 1996). These show the mechanism by which Ca and Mg carbonate salts form in solutions supersaturated with respect to these salts.



The reactions (7), (10) and (11) are used to calculate the saturation index, but it is important to mention that the carbonate activity depends on the carbonate ions equilibrium, expressed by reactions (2) to (6) as well as (8) and (9), which depend on the pH of the system. It has been reported that the presence of Mg modifies the calcium carbonate polymorph and morphology. Three polymorphs exist and these include vaterite which is usually spherical in shape, aragonite with a needle shape and calcite which has a rhombohedral shape. It is known that their stabilities increase from vaterite to aragonite to calcite. The first two phases are metastable phases, which can transform to the more stable phase calcite at room temperature (Cheng et al., 2014). The presence of other ions, particularly Mg²⁺ can have an influence on the polymorph formed, hence morphology of calcium carbonate which can also be altered due to the effect of impurity ions on the precipitation kinetics and thermodynamics. The Mg²⁺/Ca²⁺ activity ratio is important as it indicates which phase of CaCO₃ is likely to precipitate. In solutions with low Mg concentration and Mg/Ca concentration ratio <3, precipitation of calcite is both thermodynamically and kinetically favoured. With an increase in the Mg concentration beyond Mg/Ca concentration ratio of 3, aragonite precipitation is favoured instead (Rushdi, 1992; Cheng et al., 2014; Filippov et al., 2013; Wang and Mucci, 2012; Falini et al., 2009; Pokrovsky, 1998; Wang et al., 2008; Han et al., 2006; Zhou and Zheng, 2001). Moreover, the Mg²⁺ presence causes an inhibition effect on CaCO₃ growth, due to the adsorption of Mg onto calcite nuclei surfaces, which either raises the surface free energy or causes the formation of Mg-calcite carbonate of substantially higher solubility (Bischoff, 1968; Pytkowicz, 1973; Katz, 1973; Lippmann, 1973; Kitano, 1962).

The present study seeks to evaluate the removal efficiency of mineral scaling precursors from an electro dialysis concentrate in order to mitigate the scale formation in the subsequent desalination stage by evaporative crystallisation. The investigation is based on a case study of an industrial effluent, herein termed, electro dialysis concentrate (EDC) that is processed by an evaporative crystallisation pilot plant at a Brazilian oil refinery. The pre-treatment of such brines is necessary to remove scale forming metals and to improve the operational efficiency of downstream desalination processes with zero waste discharge. Prior to experimental validation, hydro-geochemical modelling was conducted and supersaturation indices calculated by PHREEQC[®] software (Parkhurst and Appelo, 2013). The model provided important parameters such as the saturation index, pH and mass yield for all the minerals likely to precipitate for each set of operational conditions under study. The experimental results were then compared to the model predictions to assess the validity of the model.

2 Methodology

2.1 Hydrogeochemical modelling

Hydrogeochemical modelling was conducted using PHREEQC Interactive[®] software version 3.1.7-9213 (Parkhurst and Appelo, 2013) in order to simulate the alkalisation of EDC. It was assumed that the chemical reactions achieved equilibrium based on the law of mass action, on the solubility product equations, as well as mass balance and charge balance for the aqueous phase. The Davies equation was used to calculate the activity coefficients of the ions in solution. The pH was controlled by varying the CO₂ concentration, since H⁺ ions can be produced by CO₂ dissolution in water according to reactions (2) to (4). The Lawrence Livermore National Laboratory database, 'lnl.dat', was used. The hydrogeochemical modelling presented the chemical composition, physical-chemical parameters of the solution and the mass yields of the solids precipitated for each chemical dosage studied.

2.2 Alkaline precipitation

Precipitation experiments were conducted using the electro dialysis concentrate from a wastewater unit in a Brazilian oil refinery. The ionic composition, total organic carbon (TOC), total dissolved solids (TDS) and pH of this stream are shown in Table 1.

Table 1 Mean chemical composition, TOC, TDS and pH of the EDC

Parameters	Total alkalinity (as CaCO ₃)	Na	Ca	Mg	SO ₄ ²⁻	Sr	Ba	TOC	TDS	pH
Values mgL ⁻¹ (except pH)	204	1008	213	53	316	10	1.3	43	354	7.6

The reactions were conducted in Pyrex/Duran[®] glass jars under stirring by means of overhead electric driven straight blade impellers. A volume of 1 litre of the EDC was added to each of the six jars for the experimental runs. Analytical grade NaOH and Ca(OH)₂ were used to adjust the pH and to achieve the precipitation conditions. The

quantities of alkaline reagent added were 0.02, 0.04, 0.06, 0.07, 0.08 and 0.09 wt.% (expressed as a fraction of the weight of EDC not the total weight after reagent addition) for both reagents in each jar separately. These were achieved by dosing the respective volumes of 8, 16, 24, 28, 32 and 36 mL of 25 gL⁻¹ Ca(OH)₂ stock solution or 5, 10, 15, 17.5, 20 and 22.5 mL of 40 gL⁻¹ NaOH aqueous solutions, which were prepared in advance and kept under agitation during pipetting. After addition of the alkaline reagent, the solutions were stirred at 300 rpm for 2 minutes followed by 100 rpm for 40 minutes. The speed was reduced in order to avoid the breakage of flocs. In sequence, the precipitate was subjected to gravitational settling for 5 minutes. The pHs of the solutions were monitored in all experiments using a Digimed pH meter. The final pHs after precipitation were in the range 9–12 for Ca(OH)₂ and 10–13 for NaOH experiments. The total dissolved solids (TDS) were determined by the correlation between TDS and conductivity.

The solids were then vacuum filtered using a 0.25 µm pore nitrocellulose/nylon membrane. The solids were dried for 24 h at 60°C in an oven. Powder X-ray diffraction (XRD) was employed to identify the crystalline phase(s) present in the solid precipitates obtained. The morphology of the precipitates was observed using scanning electron microscopy (SEM) and energy-dispersive spectroscopy (EDS) was used to obtain the surface elemental composition. The concentrations of Ca, Mg, Na, Sr and Ba in the aqueous filtrate and EDC were measured using inductively coupled plasma optical emission spectrometry (ICP-OES). The total organic carbon (TOC) and inorganic carbon (IC) in the electro dialysis concentrate (EDC) and filtrate were quantified by the oxidation method associated with catalytic combustion at temperatures of approximately 680°C and an infrared detector using the Shimadzu chromatograph, model TOC-VCPN, sampler ASI-V Shimadzu. All experiments were carried out in triplicate under room temperature of 25°C.

3 Results and discussion

3.1 Hydrogeochemical modelling and alkaline precipitation

The results obtained by PHREEQC® (Parkhurst and Appelo, 2013) calculation are coherent with experimental results where rapid precipitation of the salts occurred as indicated by the high removal efficiencies with rapid increase of pH, hence higher supersaturation (see Tables 2 and 3). The results indicate a reduction in the incrustation potential of the EDC after precipitation effected by alkaline treatment especially with caustic soda. Table 2 presents the mass yield of the mixed-solid precipitates and the final pH obtained after addition of lime and caustic soda for three experimental replicates. These are compared to the respective modelling results obtained using PHREEQC® (Parkhurst and Appelo, 2013).

A linear correlation was observed for lime experiments between the experimental mass of mixed-precipitate and the concentration of lime for both experimental and modelling results. For Ca(OH)₂ dosages greater than 0.06 wt.% (pH > 11.20), the mass of precipitate obtained was almost twice that obtained by similar NaOH dosages (pH > 12.00). However, when considering the modelling results for NaOH experiments, the mass of precipitate did not increase in accordance with experimental results and the reason for this is not quite clear. The experimental mass of solid precipitates increased

with increase in pH for both lime and NaOH experiments due to increase in the concentration of OH^- ions in solution, thereby increasing the supersaturation. Whilst calcium forms more insoluble salts when compared to sodium, the higher precipitate mass obtained with $\text{Ca}(\text{OH})_2$ is attributed mainly to precipitation of the added Ca^{2+} ions in addition to the Ca^{2+} already present in solution. This is supported by the fact that addition of $\text{Ca}(\text{OH})_2$ resulted in final solution concentrations that were higher than those obtained with NaOH despite having a higher precipitate mass (see Table 2). In addition, for both lime and caustic soda, alkaline dosages of 0.04 wt.% raised the pH to 10 and higher, whereby the CO_3^{2-} ion is predominant in solution and these favours the precipitation of carbonate salts such as calcium carbonate.

Table 2 Mass of solids precipitated and pH obtained

Reagent/ Solution ratio [wt.%]	Mass of precipitate [g]		pH [45 min]		
	Modelling	Experimental	Modelling	Experimental	
Lime ($\text{Ca}(\text{OH})_2$)	0.02	0.25	0.20 ± 0.01	8.83	8.73 ± 0.16
	0.04	0.52	0.42 ± 0.01	9.58	9.19 ± 0.19
	0.06	0.64	0.55 ± 0.02	11.20	11.28 ± 0.13
	0.07	0.76	0.60 ± 0.02	11.29	11.50 ± 0.08
	0.08	0.84	0.62 ± 0.02	11.43	11.65 ± 0.11
	0.09	0.94	0.67 ± 0.02	11.53	11.85 ± 0.20
Caustic soda (NaOH)	0.02	0.23	0.13 ± 0.03	9.62	9.77 ± 0.19
	0.04	0.11	0.42 ± 0.09	11.72	11.20 ± 0.34
	0.06	0.11	0.36 ± 0.01	11.97	12.08 ± 0.25
	0.07	0.11	0.35 ± 0.01	12.05	12.15 ± 0.25
	0.08	0.11	0.38 ± 0.01	12.12	12.30 ± 0.22
	0.09	0.11	0.35 ± 0.01	12.18	12.48 ± 0.27

The TDS decreased very slightly with increase in lime concentration while it increased with increase in NaOH concentration as shown in Figure A.1 in the supporting information. The slight decrease in TDS caused by lime is due to precipitation of some or all of the added Ca^{2+} and OH^- ions accompanied by solution volume reduction while the increase in TDS caused by NaOH is due to increase in the concentration of a non-precipitating ion, Na^+ .

The total organic carbon (TOC) remained almost constant in the range 33 to 41 mgL^{-1} with increase in alkaline reagent concentration (Figure 1) indicative of null degradation or removal of organic compounds from the EDC which ranges from 33 to 41 mgL^{-1} . This organic content is responsible for the formation of foam in the evaporative crystalliser, which disturbs the operations of the process. It is verified that the organic contaminants (polymeric electrolytes possessing acidic oxygen-containing residues such as phenol group (Becheleni et al., 2014) cannot be removed by coprecipitation or adsorption onto CaCO_3 (Effenberger et al., 1981). On the other hand, as expected, the inorganic carbon (IC) concentration in aqueous solution decreased with the increase in alkaline concentration. The reduction in IC obtained lime was ca. 80% and 96% for dosages of 0.04 and 0.06 wt.%, respectively, while for caustic soda addition, the reduction was ca. 90% for alkaline dosages > 0.04 wt.%, see Figure 1. However, the discrepancies observed

between lime and caustic soda could be possibly due to analytical errors since the standard deviations of the final concentration values overlap for both alkaline reagents. The IC concentration reduction in solution also confirms the precipitation of carbonates.

Figure 1 Total organic carbon (TOC) and inorganic carbon (IC) concentrations profiles

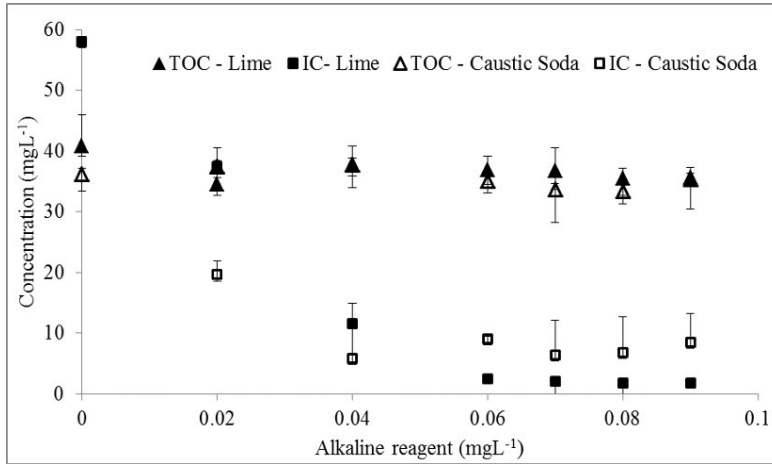


Table 3 Removal of metals from electro dialysis concentrate (EDC) and pH of solutions after 45 minutes of experiment

Reagent/ Solution ratio [wt.%]	Removal [%]				pH (45min)	
	Ca	Mg	Ba	Sr		
Lime	0.02	33.8	1.28	41.5	21.3	8.73 ± 0.16
	0.04	41.9	1.68	48.9	26.00	9.19 ± 0.19
	0.06	43.9	28.67	58.5	30.1	11.28 ± 0.13
	0.07	43.7	58.69	62.2	33.1	11.50 ± 0.08
	0.08	42.1	93.10	63.0	33.1	11.65 ± 0.11
	0.09	38.5	99.08	62.2	32.6	11.85 ± 0.20
Caustic soda	0.02	37.4	20.4	63.0	34.6	9.77 ± 0.19
	0.04	>99.8	76.2	89.6	85.0	11.20 ± 0.34
	0.06	>99.8	99.6	91.1	83.3	12.08 ± 0.25
	0.07	>99.8	99.8	78.5	59.2	12.15 ± 0.25
	0.08	>99.8	99.9	80.7	61.6	12.30 ± 0.22
	0.09	>99.8	99.9	84.4	66.5	12.48 ± 0.27

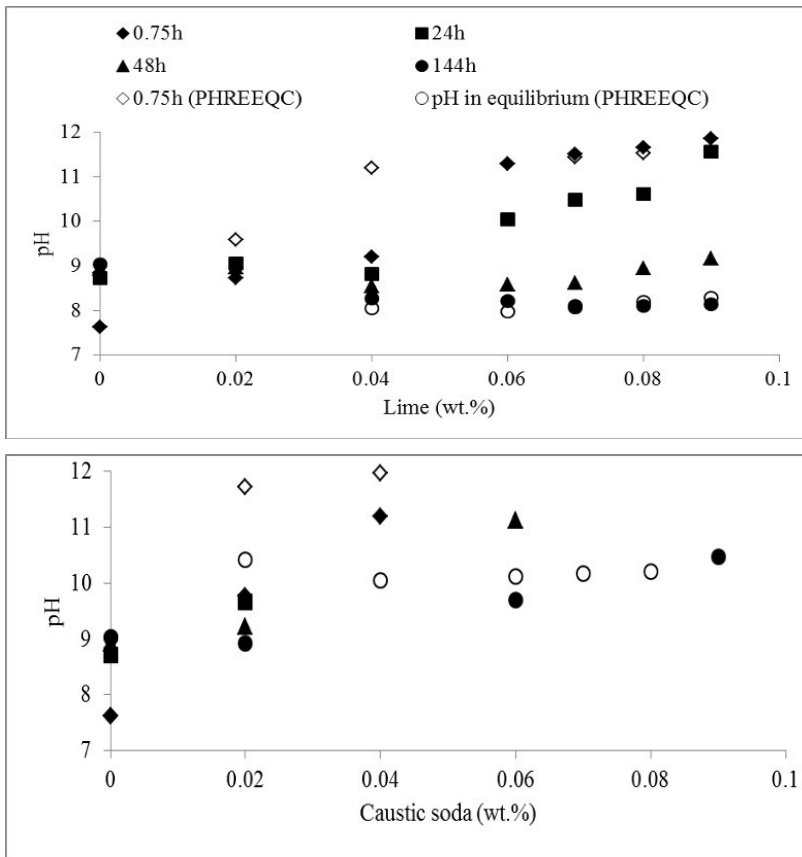
Table 3 shows the percentage reduction in the quantities of scale-forming metal ions. Alkaline precipitation of salts from electro dialysis concentrate caused a reduction in the concentrations of Ca (44%), Mg (29%), Ba (59%) and Sr (30%) in solution when lime was used as the alkaline reagent at a concentration of 0.06 wt.%. The dosage of up to 0.04 wt.% of caustic soda achieved a calcium reduction of >99.8%. A magnesium removal of 76% to 99.6% was achieved with dosages of 0.04–0.06 wt.% NaOH. It is also important to highlight the barium concentration reduction of 63 to 90% and a maximum

of 85% of strontium removal for a dosage of 0.04 wt.% NaOH, since they are scale forming elements. It is observed that Ca(OH)₂ addition caused the biggest precipitation in mass, since the calcium added also precipitates, while NaOH addition was more efficient for Ca removal (see Figure 3 and Tables 3 and 4). Table 4 shows the final Ca concentrations attained for both lime and caustic soda experiments.

Table 4 Final Ca concentrations attained

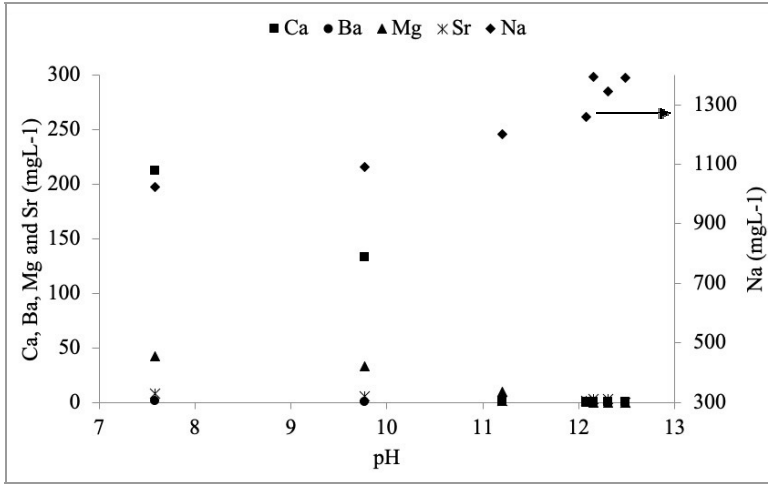
Reagent/ Solution ratio [wt.%]	Lime experiments Ca (mgL ⁻¹)	Caustic soda experiments Ca (mgL ⁻¹)
0.00	212.53 ± 34.91	212.53 ± 34.91
0.02	140.62 ± 36.61	133.03 ± 18.60
0.04	123.52 ± 30.36	Not detected
0.06	119.32 ± 28.96	Not detected
0.07	119.67 ± 34.46	Not detected
0.08	123.14 ± 39.28	Not detected
0.09	130.71 ± 45.19	Not detected

Figure 2 Mean pH values as a function of time for lime and caustic soda additions

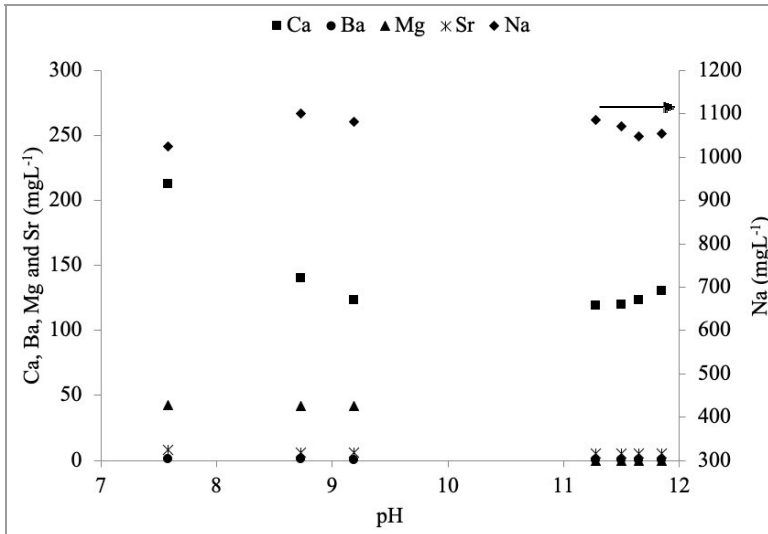


During the precipitation experiments, the pH was monitored for all dosages of lime and caustic soda (Figure 2). It was noted that the pH increased from its initial value (7.58) to the equilibrium point as predicted by PHREEQC[®] modelling (Parkhurst and Appelo, 2013).

Figure 3 Variation of the final metal concentrations in solution with pH for (a) caustic soda and (b) lime



(a)



(b)

The pH stabilised around 8 for lime addition [Figure 3(a)] and approximately 10 for caustic soda addition after 144 hours in agreement with the final pH value predicted by PHREEQC[®]. The pH values obtained after stabilising for 48 hours are almost close to the equilibrium values especially for lime experiments, showing that near-equilibrium conditions can be attained within 48 hours. Upon addition of 0.04 wt.% of caustic soda

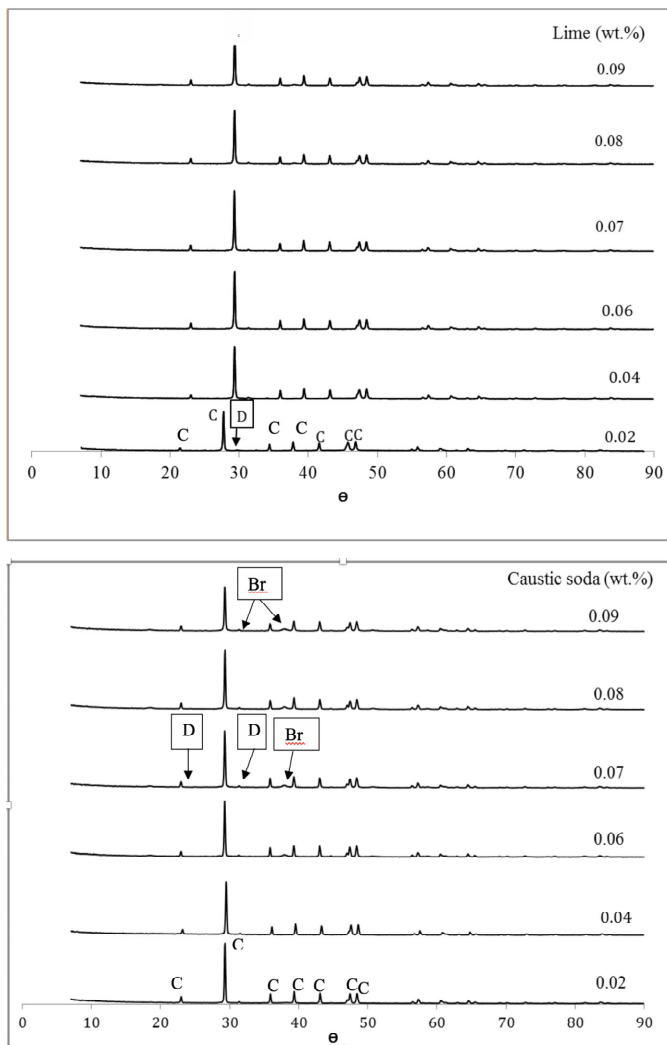
solution for 0.75 h, the pH increased to ca. 11, causing the formation of carbonate solids with less reagent consumption compared to lime which required 0.06 wt.% to achieve the corresponding pH. This is confirmed by the high removal efficiencies of Ca and Mg upon addition of 0.04 wt.% of NaOH reagent (Table 3). Figure 3 presents the variation of the concentration of metals (Ca, Ba, Mg, Sr and Na) in solution with pH. An abrupt reduction in calcium and magnesium content upon adding NaOH reagent solution was observed [Figure 3(a)], at pH of about 11, achieving concentration levels below the detection limit of ICP-OES. In contrast, for the same pH condition in the case of lime, calcium concentration starts to increase [Figure 3(b)]. This could be due to the onset of Mg salt precipitation, possibly $\text{Mg}(\text{OH})_2$, shown by the sudden reduction in Mg concentration upon increasing the pH from ca. 9 to above 11, notable for both alkaline reagents. However, it is postulated that the plateauing and subsequent increase in Ca concentration observed for lime arises from the continual addition of Ca ions, whose hydroxide and carbonate precipitation is likely suppressed at $\text{pH} > 9$ due to precipitation of $\text{Mg}(\text{OH})_2$. In support of this postulation, Gabelich et al. (2007) reported that $\text{Mg}(\text{OH})_2$ becomes supersaturated at $\text{pH} > 10$ while $\text{Ca}(\text{CO}_3)$ which attains supersaturation at lower $\text{pH} > 6.5$ tends to constant supersaturation at $\text{pH} > 10$ as pH is increased. On the contrary, the Ca concentration continued to decrease with increase in pH for caustic soda since there were no Ca^{2+} ions introduced in the system. These results indicate that the addition of 0.04 wt.% of caustic soda is optimal for removal of low solubility salts from the reverse electro dialysis concentrate.

3.2 Solid phases precipitated

Figure 4 shows the XRD diffractograms of the mixed precipitate samples obtained at different lime and caustic soda dosages. The phases predicted by modelling and those obtained experimentally, as confirmed by XRD, are in concordance. However, not all the phases indicated by modelling were exactly obtained experimentally because PHREEQC® (Parkhurst and Appelo, 2013) does not consider the reaction kinetics.

Calcite (CaCO_3) and dolomite ($\text{CaMg}(\text{CO}_3)_2$) are obtained both, theoretically and experimentally as presented in the diffractograms in Figure 4. However, calcium carbonate can be considered as the main low solubility salt and precursor of scaling on evaporative crystalliser walls since it is the most frequent phase shown by the diffractograms (Figure 4). Powder XRD characterisation confirmed the formation of calcite as the main phase formed for all experimental conditions. Brucite, $\text{Mg}(\text{OH})_2$, was detected in some experimental conditions with very low intensity peaks, as depicted in Figure 4. At a caustic soda concentration of 0.04 wt.%, $\text{CaMg}(\text{CO}_3)_2$ was the main phase indicated by XRD and since its peaks are almost coincident with those of the calcite phase, it is reasonable to consider co-precipitation of Mg with the calcite phase. Gabelich et al. (2007) also identified calcite and brucite in their solid precipitates.

The precipitated phases are also in agreement with those obtained by Santos et al. (2017) upon injection of carbon dioxide into the same stream as the one used in the present work, whereby the authors identified CaCO_3 and $\text{Mg}(\text{OH})_2$ as the major phases formed at 35°C . The presence of precipitates with the dolomite crystal structure [e.g., calcite and magnesite according to Effenberger et al. (1981)] was expected to be the third main type of salts.

Figure 4 X-ray diffractograms of the mixed-solid precipitates for lime and caustic soda additions

Note: Calcite – CaCO_3 (C), dolomite – $\text{CaMg}(\text{CO}_3)_2$ (D) and brucite – $\text{Mg}(\text{OH})_2$ (Br)

As the Mg/Ca activity ratio of the solution rises, eventually dolomite saturation is reached after calcite and magnesium hydroxide precipitation. The difficulty of dolomite formation from saline solution is related to the rapid carbonate precipitation rate of metastable phases, which consumes the calcium and magnesium ions and the high hydration energy of the magnesium ion (Rushdi, 1992). This probably hinders the formation of dolomite first in the saline solution due to the low Mg/Ca initial ratio of about 0.23 in the electro dialysis concentrate. This ratio becomes even lower after lime addition in the beginning of the precipitation. Also, as mentioned before, the Arrhenius activation energy for dolomite is in the range of 12–38 kcal mol⁻¹ (Busenberg and Plummer, 1982), a superior value compared with that of calcite, around 10 kcal mol⁻¹ (Plummer et al., 1978; Nancollas and Reddy, 1971; Wiechers et al., 1975; Kazmierczak et al., 1982) and brucite, 10 kcal mol⁻¹ (Pokrovsky and Schott, 2004; Vermilyea, 1969; Mejjas et al., 1999).

Reaction rates are dependent on temperature, grain size, diffusion transport and sites of nucleation at borders (Carlson and Gordon, 2004; Hacker et al., 2005). Dolomite can be formed at low temperatures as disordered dolomite (Montes-Hernandez et al., 2016). In natural conditions, the formation of dolomite at ambient temperature is virtually impossible. According to Montes-Hernandez et al. (2014), 50% ordered dolomite required about 90 days at 200°C to be formed. Actually, at ambient temperature, high magnesium-bearing calcite is precipitated first, acting as a precursor for dolomite formation maintaining a constant carbonate alkalinity.

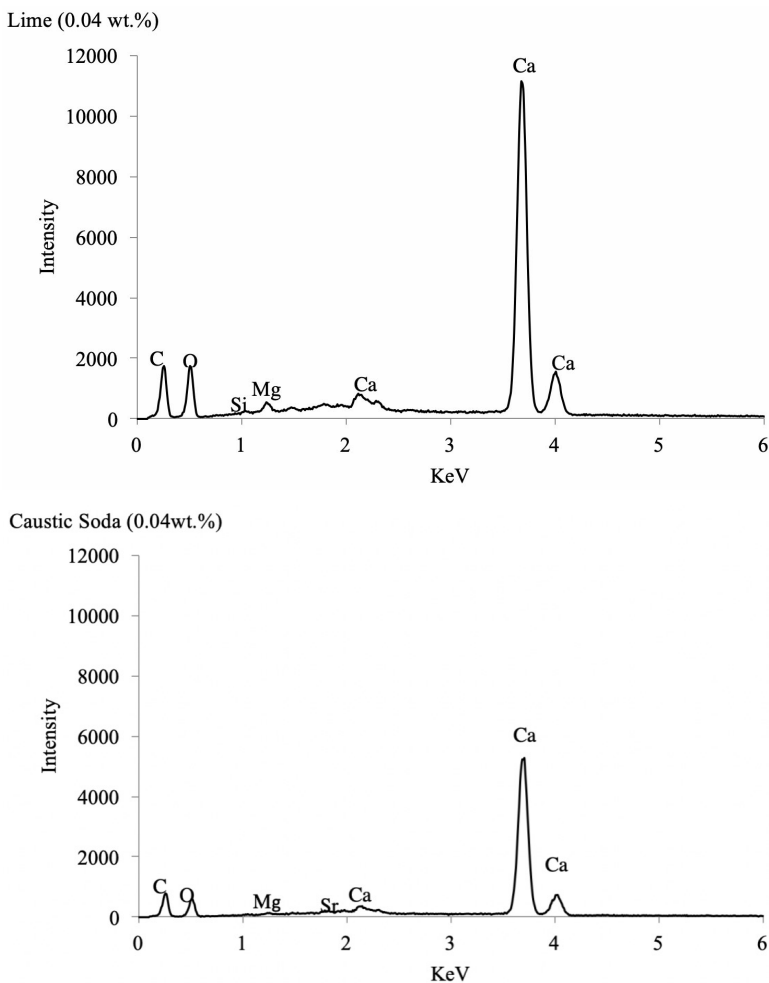
Davis et al. (2011) investigated the growth kinetics of dolomite and calcite at 800°C. The rate constant for the growth of dolomite was about $10^{-5} \mu\text{m}^3 \text{s}^{-1}$, according to the authors, which were four orders of magnitude smaller than that of calcite ($0.1 \mu\text{m}^3 \text{s}^{-1}$). In addition, the highest rate constant of calcite growth is obtained when there is extensive Mg substitution for Ca, while dolomite has the lowest growth rate constant at insignificant concentration of Mg in solution.

As noted in Figure 4, in the case of alkalisation using caustic soda, calcite was the more frequent phase obtained under all experimental conditions except for the experiments with ≥ 0.04 wt.% caustic soda where $\text{CaMg}(\text{CO}_3)_2$ was also detected; possibly this phase corresponds to a high magnesium-bearing calcite phase. $\text{Mg}(\text{OH})_2$ was only detected by XRD at caustic soda dosages of greater or equal to 0.06 wt.%. The precipitation of $\text{Mg}(\text{OH})_2$, CaCO_3 and $\text{CaMg}(\text{CO}_3)_2$ was predicted by the hydrogeochemical modelling software, but it does not consider the kinetics of these reactions.

3.3 Solids qualitative elemental composition and morphology

Figure 5 shows the elemental composition of the precipitates obtained from experiments conducted with 0.04 wt.% of lime and caustic soda, as detected by EDS. The semi-qualitative elemental composition obtained reveals high levels of calcium (Ca), medium quantities of carbon (C) and oxygen (O) and very low amounts of magnesium (Mg), silicon (Si) and strontium (Sr). This confirms the predominance of calcium and magnesium bearing carbonate/hydroxide salts, followed by magnesium hydroxide as solid precipitates for both cases.

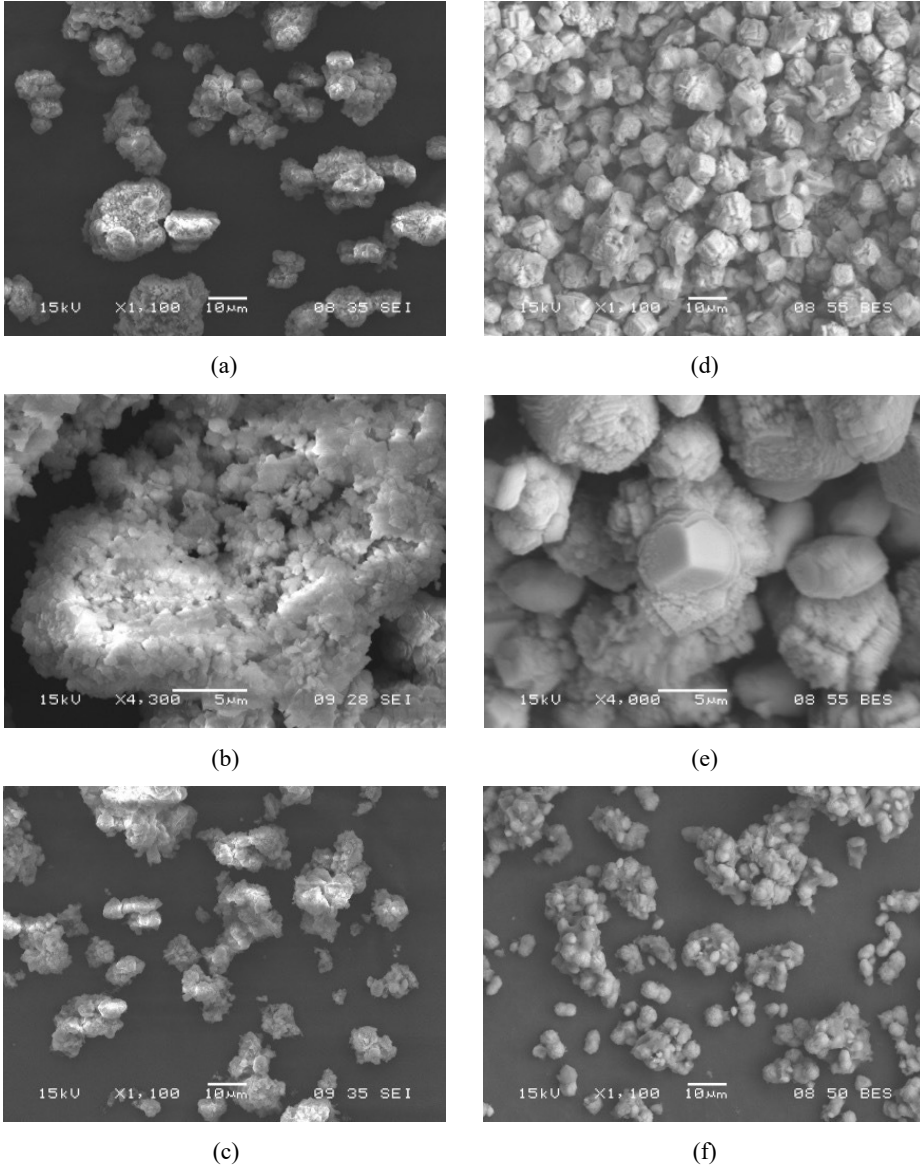
Figures 6(a) to 6(f) present the size and morphology of the precipitates formed in lime and caustic soda experiments (0.04 wt.% and 0.09 wt.%). The particle sizes of the precipitates decreased with an increase in alkaline dosage due to increased supersaturation which favoured nucleation over growth [compare Figure 6(a) with Figure 6(c) for lime dosages of 0.04 and 0.09 wt.%, respectively, and Figure 7(d) with Figure 7(f) for the corresponding caustic soda dosages). Moreover, the proportion of smaller particles ($<1 \mu\text{m}$) identified in agglomerates was much higher for lime experiments than for caustic soda experiments, see Figures 6(b) and 6(E), respectively. The later had some well-faceted crystals of sizes greater than $5 \mu\text{m}$. The higher supersaturation associated with lime addition therefore favours nucleation over growth and promotes secondary processes such as aggregation and agglomeration.

Figure 5 SEM EDS analyses of precipitates obtained by dosing 0.04wt.% of lime and caustic soda

The precipitates formed in both lime and caustic soda experiments were agglomerates of crystals with rhombohedral morphology, typical of calcite, as presented in Figure 6. Rhombohedral calcite particles in the aggregates [Figure 6(b)] as well as slightly elongated particles, typical of aragonite [Figure 6(f)] are morphologies commonly reported for calcium carbonate particles in the presence of magnesium (Zhou and Zheng, 2001). It is possible that with increase in the alkaline reagent concentration, the metastable phase, vaterite, could have precipitated, hence some spherical shapes. However, direct detection of the polymorphs by powder XRD was difficult due to presence of a mixture of precipitates in this case. Various authors have reported that calcium carbonate morphology is susceptible to many factors especially pH, temperature, supersaturation and presence of impurities (Rushdi, 1992; Cheng et al., 2014; Filippov et al., 2013; Wang and Mucci, 2012; Liu et al., 2011; Falini et al., 2009; Wang et al., 2008; Han et al., 2006; Zhou and Zheng, 2001). As reported by Wang et al. (2008), the morphology transition of CaCO_3 may also be related to an increase in Ca concentration.

Figure 6(e) also shows a multistep aggregation mechanism of calcium carbonate particles most likely as calcite and vaterite, according to Zhou and Zheng (2001) in aqueous solution as shown by the progressively increasing sizes of the aggregates with flower, elongated and rhombohedral shapes.

Figure 6 Solid precipitates after addition of lime [(a)-(b) 0.04 wt.% (c) 0.09 wt.%] and caustic soda [(d)-(e) 0.04 wt.% (f) 0.09 wt.%]



The precipitates obtained by alkaline precipitation may be indispensable in the evaporative crystallisation pilot plant as seeds. This would promote secondary nucleation of sparingly soluble salts in the bulk of the solution rather than nucleation on the

crystalliser walls, thereby minimising scaling and substantially improving NaCl removal from the EDC.

4 Conclusions

In this work, pre-treatment of an electro dialysis concentrate (EDC) by alkaline precipitation using lime and caustic soda reagents has been presented with the aim to minimise scale formation in the downstream evaporative crystallisation process. It has been demonstrated that alkaline precipitation was an effective method for removing scale-forming salts such as calcium carbonate and magnesium hydroxide from the reverse electro dialysis concentrate. The highest removal of Ca was achieved by addition of 0.04 wt.% of caustic soda, with a Ca reduction of 99.8% and a Mg reduction of 76.2% from the saline concentrate. The Mg removal increased to 99.6% upon increasing the dosage of caustic soda to 0.06 wt.%.

The results obtained by modelling with PHREEQC[®] were consistent with the experimental results obtained. The results indicate a reduction in the incrustation potential of electro dialysis concentrate after precipitation effected by alkaline treatment, especially with caustic soda. Powder XRD and SEM-EDS also confirmed the dominance of calcium and magnesium species in the solid precipitates, which are the two main scale forming metals in the EDC.

The removal of calcium and magnesium from the electro dialysis concentrate would reduce the formation of mineral scale during the downstream evaporative crystallisation process. It is recommended to use a portion of the precipitate obtained during the pre-treatment process for seeding in the evaporative crystallisation process. This would promote secondary nucleation in the bulk solution and further reduce nucleation, hence scale formation on the crystalliser walls.

Acknowledgements

The authors wish to acknowledge PETROBRAS, CAPES, FAPEMIG and CNPq (Process number 308044/2018-5) for their financial support and also to the Center of Microscopy at the Universidade Federal de Minas Gerais (<http://www.microscopia.ufmg.br>) for providing the equipment and technical support for experiments involving electron microscopy.

References

- Adams, J.F. and Papangelakis, V.G. (2000) 'Gypsum scale formation in continuous neutralization reactors', *Canadian Metallurgical Quarterly*, Vol. 39, No. 4, pp.421–432 [online] <https://doi.org/10.1179/cmqr.2000.39.4.421>.
- Andreassen, J.P. (2005) 'Formation mechanism and morphology in precipitation of vaterite – nano-aggregation or crystal growth', *Journal Crystal Growth*, Vol. 274, Nos. 1–2, pp.256–264 [online] <https://doi.org/10.1016/j.jcrysro.2004.09.090>.
- Becheleni, E.M.A., Borba, R.P., Seckler, M.M. and Rocha, S.D.F. (2014) 'Water recovery from saline streams produced by electro dialysis', *Environmental Technology*, Vol. 36, No. 3, pp.386–394 [online] <https://doi.org/10.1080/09593330.2014.978898>.

- Betrie, G.D., Sadiq, R., Nichol, C., Morin, K.A. and Tesfamariam, S. (2016) 'Environmental risk assessment of acid rock drainage under uncertainty: the probability bounds and PHREEQC approach', *Journal Hazardous Materials*, Vol. 301, pp.187–196 [online] <https://doi.org/10.1016/j.jhazmat.2015.07.022>.
- Bischoff, J.L. (1968) 'Kinetics of calcite nucleation: magnesium ion inhibition and ionic strength catalysis', *Journal of Geophysical Research*, Vol. 73, No. 10, pp.3313–3322 [online] <https://doi.org/10.1029/JB073i010p03315>.
- Blue, C.R. and Dove, P.M. (2015) 'Chemical controls on the magnesium content of amorphous calcium carbonate', *Geochimica et Cosmochimica Acta*, Vol. 148, pp.23–33 [online] <https://doi.org/10.1016/j.gca.2014.08.003>.
- Busenberg, E. and Plummer, L.N. (1982) 'The kinetics of dissolution of dolomite in CO₂-H₂O systems at 1.5 to 65°C and 0 to 1 atm P_{CO₂}', *American Journal of Science*, Vol. 282, No. 1, pp.45–78 [online] <http://pubs.er.usgs.gov/publication/70011818>.
- Carlson, W.D. and Gordon, C.L. (2004) 'Effects of matrix grain size on the kinetics of intergranular diffusion', *Journal of Metamorphic Geology*, Vol. 22, No. 8, pp.733–742 [online] <https://doi.org/10.1111/j.1525-1314.2004.00545.x>.
- Charlton, S.R. and Parkhurst, D.L. (2011) 'Modules based on the geochemical model PHREEQC for use in scripting and programming languages', *Computers & Geosciences*, Vol. 37, No. 10, pp.1653–1663 [online] <https://doi.org/10.1016/j.cageo.2011.02.005>.
- Chaussemier, M., Pourmohtashama, E., Gelus, D., Pécou, N., Perrot, H., Lédion, J., Cheap-Charpentier, H. and Horner, O. (2015) 'State of art of natural inhibitors of calcium carbonate scaling. a review article', *Desalination*, Vol. 356, pp.47–55 [online] <https://doi.org/10.1016/j.desal.2014.10.014>.
- Cheng, H., Zhang, X. and Song, H. (2014) 'Morphological investigation of calcium carbonate during ammonification-carbonization process of low concentration calcium solution', *J. Nanomaterials*, Vol. 2014, Article ID 503696, 7pp.
- Davis, N.E., Newman, J., Wheelock, P.B. and Kronenberg, A.K. (2011) 'Grain growth kinetics of dolomite, magnesite and calcite: a comparative study', *Physic and Chemistry Minerals*, Vol. 38, pp.123–138 [online] <https://doi.org/10.1007/s00269-010-0389-9>.
- Effenberger, H., Mereiter, K. and Zemann, J. (1981) 'Crystal structure refinements of magnesite, calcite, rhodochrosite, siderite, smithonite, and dolomite, with discussion of some aspects of the stereochemistry of calcite type carbonates', *Zeitschrift fur Kristallographie*, Vol. 156, pp.233–243.
- Falini, G., Fermani, S., Tosi, G. and Dinelli, E. (2009) 'Calcium carbonate morphology and structure in the presence of seawater ions and humic acids', *Crystal Growth & Design*, Vol. 9, No. 5, pp.2065–2072.
- Faux, R.F., Busenberg, E. and Plummer, L.N. (1986) 'The dissolution kinetics of magnesite from 25–85°C and pH's of 0 to 10 at atmospheric P_{CO₂}', *Geological Society of America*, Vol. 18, No. 6, p.599.
- Filippov, L.O., Grandjean, M., Filippov, A.I.V. and Pelletier, M. (2013) 'Morphology of carbonates particles precipitation from saline waste solution: influence of magnesium', *Journal of Physics*, Vol. 416, pp.1–6 [online] <https://doi.org/10.1088/1742-6596/416/1/012011>.
- Gabelich, C.J., Rahardianto, A., Northrup, C.R., Yun, T.I. and Cohen, Y. (2011) 'Process evaluation of intermediate chemical demineralization for water recovery enhancement in production-scale brackish water desalting', *Desalination*, Vol. 272, Nos. 1–3, pp.36–45 [online] <https://doi.org/10.1016/j.desal.2010.12.050>.
- Gabelich, C.J., Williams, M.D., Rahardianto, A., Franklin, J.C. and Cohen, Y. (2007) 'High-recovery reverse osmosis desalination using intermediate chemical demineralization', *Journal of Membrane Science*, Vol. 301, No. 1, pp.131–141 [online] <https://doi.org/10.1016/j.memsci.2007.06.007>.
- Greenlee, L.F., Lawler, D.F., Freeman, B.D., Marrot, B., Moulin, P. (2009) 'Reverse osmosis desalination: water sources, technology and today's challenges', *Water Research*, Vol. 43, Nos. 1–2, pp.2317–2348 [online] <https://doi.org/10.1016/j.memsci.2007.06.007>.

- Hacker, B.R., Rubie, D.C., Kirby, S.H. and Bohlen, S.R. (2005) 'The calcite, aragonite transformation in low-Mg marble: equilibrium relations, transformation mechanisms, and rates', *Journal of Geophysical Research*, Vol. 110, No. B3, p.B03205.
- Han, Y.S., Hadiko, G., Fuji, M. and Takahashi, M. (2006) 'Crystallization and transformation of vaterite at controlled pH', *Journal of Crystal Growth*, Vol. 289, No. 1, pp.269–274 [online] <https://doi.org/10.1016/j.jcrysgro.2005.11.011>.
- Harvie, C.E. and Weare, J.H. (1989) 'The prediction of mineral solubilities in natural waters: the Na-K-Mg-Ca-Cl-SO₄-H₂O system from zero to high concentration at 25°C', *Geochimica et Cosmochimica Acta*, Vol. 53, No. 10, pp.2503–2518 [online] [https://doi.org/10.1016/0016-7037\(89\)90124-5](https://doi.org/10.1016/0016-7037(89)90124-5).
- Hoang, T.A., Ang, H.M. and Rohl, A.L. (2004) 'Development of a laboratory experimental system for studying gypsum scale formation in pipes', Paper presented at the *10th Asian Pacific Confederation of Chemical Engineering*, Kitakyushu, Japan.
- Hoang, T.A., Ang, H.M. and Rohl, A.L. (2007) 'Effects of temperature on the scaling of calcium sulphate in pipes', *Powder Technology*, Vol. 179, pp.31–37.
- Katz, A. (1973) 'The interaction of magnesium with calcite during crystal growth at 25–90°C and one atmosphere', *Geochimica et Cosmochimica Acta*, Vol. 37, No. 6, pp.1563–1586 [online] [https://doi.org/10.1016/0016-7037\(73\)90091-4](https://doi.org/10.1016/0016-7037(73)90091-4).
- Kazmierczak, T.F., Tomson, M.B. and Nanchollas, G.H. (1982) 'Crystal growth of calcium carbonate: a controlled composition kinetic study', *Journal of Physical Chemistry*, Vol. 86, No. 1, pp.103–107 [online] <https://doi.org/10.1021/j100390a020>.
- Kim, D.H. (2011) 'A review of desalting process techniques and economic analysis of the recovery of salts from Retentates', *Desalination*, Vol. 270, Nos. 1–3, pp.1–8 [online] <https://doi.org/10.1016/j.desal.2010.12.041>.
- Kitano, Y. (1962) 'The behavior of various inorganics ions in the separation of calcium carbonate from a bicarbonate solution', *Bulletin of Chemical Society of Japan*, Vol. 35, No. 12, pp.1973–1980 [online] <https://doi.org/10.1246/bcsj.35.1973>.
- Lewis, A.E., Nathoo, J., Thomsen, K., Kramer, H.J.M., Witkamp, G.J., Reddy, S.T. and Randall, D.G. (2010) 'Design of a eutectic freeze crystallization process for multicomponent wastewater stream', *Chemical Engineering Research and Design*, Vol. 88, No. 9, pp.1290–1296 [online] <https://doi.org/10.1016/j.cherd.2010.01.023>.
- Liao, M.Y. and Randtke, S.J. (1986) 'Predicting the removal of soluble organic contaminants by lime softening', *Water Research*, Vol. 20, No. 1, pp.27–35 [online] [https://doi.org/10.1016/0043-1354\(86\)90210-1](https://doi.org/10.1016/0043-1354(86)90210-1).
- Lippmann, F. (1973) *Sedimentary Carbonate Minerals*, Springer-Verlag, New York.
- Liu, D., Hui, F., Ledion, J. and Li, F.F. (2011) 'Study of the scaling formation mechanism in recycling water', *Environmental Technology*, Vol. 33, No. 9, pp.1017–1030 [online] <https://doi.org/10.1080/09593330.2010.523438>.
- Macedonio, F., Katzir, L., Geisma, N., Simone, S., Drioli, E. and Gilron, J. (2011) 'Wind-aided intensified evaporation (WAIV) and membrane crystallizer (Mcr) integrated brackish water desalination process: advantages and drawbacks', *Desalination*, Vol. 273, No. 1, pp.127–135 [online] <https://doi.org/10.1016/j.desal.2010.12.002>.
- Mejias, J.A., Berry, A.J., Refson, K. and Fraser, D.G. (1999) 'The kinetics and mechanism of MgO dissolution', *Chemical Physics Letters*, Vol. 314, Nos. 5–6, pp.558–563 [online] [https://doi.org/10.1016/S0009-2614\(99\)00909-4](https://doi.org/10.1016/S0009-2614(99)00909-4).
- Mezher, T., Fath, H., Abbas, Z. and Khaled, A. (2011) 'Techno-economic assessment and environmental impacts of desalination technologies', *Desalination*, Vol. 2666, Nos. 1–3, pp.263–273 [online] <https://doi.org/10.1016/j.desal.2010.08.035>.
- Montes-Hernandez, G., Findling, N. and Renard, F. (2016) 'Dissolution-precipitation reactions controlling fast formation of dolomite under hydrothermal conditions', *Applied Geochemistry*, Vol. 73, pp.169–177 [online] <https://doi.org/10.1016/j.apgeochem.2016.08.011>.

- Montes-Hernandez, G., Findling, N., Renard, F. and Auzende, A.L. (2014) 'Precipitation of ordered dolomite via simultaneous dissolution of calcite and magnesite: new experimental insights into an old precipitation enigma', *Crystal Growth Design*, Vol. 14, No. 2, pp.671–677 [online] <https://doi.org/10.1021/cg401548a>.
- Morillo, J., Usero, J., Rosado, D., El Bacuori, H., Riaza, A. and Bernaola, F.J. (2014) 'Comparative study of brine management technologies for desalination plants', *Desalination*, Vol. 336, pp.32–49 [online] <https://doi.org/10.1016/j.desal.2013.12.038>.
- Mullin, J.W. (2001) *Crystallization*, 5th ed., Butterworth-Heinemann London.
- Mutamim, N.S.A., Noor, Z.Z., Hassan, M.A.A. and Olsson G. (2012) 'Application of membrane bioreactor technology in treating high strength industrial wastewater: a performance review', *Desalination*, Vol. 305, pp.1–11 [online] <https://doi.org/10.1016/j.desal.2012.07.033>.
- Nancollas, G.H. and Reddy, M.M. (1971) 'The crystallization of calcium carbonate, ii calcite growth mechanism', *Journal of Colloid Interface Science*, Vol. 37, No. 4, pp.824–830 [online] [https://doi.org/10.1016/0021-9797\(71\)90363-8](https://doi.org/10.1016/0021-9797(71)90363-8).
- Nehrke, G. and Cappellen, P.V. (2006) 'Framboidal vaterite aggregates and their transformation into calcite: a morphological study', *Journal of Crystal Growth*, Vol. 287, No. 1, pp.528–530 [online] <https://doi.org/10.1016/j.jcrysgro.2005.11.080>.
- Parkhurst, D.L. and Appelo, C.A.J. (2013) 'Description of input and examples for PHREEQC version 3 – a computer program for speciation batch-reaction one-dimensional transport and inverse geochemical calculations', *US Geological Survey Techniques and Methods*, Book 6, Chapter A43, 497pp [online] <http://pubs.usgs.gov/tm/06/a43> (accessed 25 March 2018).
- Pitzer, K.S. (1979) 'Theory-ion interaction approach', in Pytkowicz, R.M. (Ed.): *Activity Coefficients in Electrolyte Solutions*, pp.157–208, CRC Press, Inc., Boca Raton, Florida.
- Plummer, N.L., Wigley, T.M.L. and Parkhurst, D.L. (1978) 'The kinetics of calcite dissolution in CO₂-water systems at 5 to 60°C and 0.0 to 1 atm CO₂', *American Journal of Science*, Vol. 278, No. 2, pp.179–216 [online] <https://doi.org/10.2475/ajs.278.2.179>.
- Pokrovsky, O.S. (1998) 'Precipitation of calcium and magnesium carbonates from homogeneous supersaturated solution', *Journal of Crystal Growth*, Vol. 186, Nos. 1–2, pp.233–239 [online] [https://doi.org/10.1016/S0022-0248\(97\)00462-4](https://doi.org/10.1016/S0022-0248(97)00462-4).
- Pokrovsky, O.S. and Schott, J. (2004) 'Experimental study of brucite dissolution and precipitation in aqueous solution: surface speciation and chemical affinity control', *Geochemica et Cosmochemica Acta*, Vol. 68, No. 1, pp.31–45 [online] [https://doi.org/10.1016/S0016-7037\(03\)00238-2](https://doi.org/10.1016/S0016-7037(03)00238-2).
- Pytkowicz, R.M. (1973) 'Calcium carbonate retention in supersaturated seawater', *American Journal of Science*, Vol. 273, No. 6, pp.515–522 [online] <https://doi.org/10.2475/ajs.273.6.515>.
- Qu, D., Wanga, J., Wang, L., Hou, D., Luan, Z. and Wang, B. (2009) 'Integration of accelerated precipitation softening with membrane distillation for high-recovery desalination of primary reverse osmosis concentrate', *Separation and Purification Technology*, Vol. 67, No. 1, pp.21–25 [online] <https://doi.org/10.1016/j.seppur.2009.02.021>.
- Reddy, S.T., Lewis, A.E., Witkamp, G.J., Kramer, H.J.M. and Van Spronsen, J. (2010) 'Recovery of Na₂SO₄·10H₂O from a reverse osmosis retentate by eutectic freeze crystallization technology', *Chemical Engineering Research and Design*, Vol. 88, No. 9, pp.1153–1157 [online] <https://doi.org/10.1016/j.chemd.2010.01.010>.
- Rock, P.A., Mandell, G.K., Casey, W.H. and Walling E.M. (2001) 'Electrochemical cell measurements and theoretical calculations', *American Journal of Science*, Vol. 301, No. 2, pp.103–111 [online] <https://doi.org/10.2475/ajs.301.2.103>.
- Rushdi, A.I. (1992) 'Mineralogy and morphology of calcium carbonate as a function of magnesium concentration in artificial seawater', *Arabian Journal of Geoscience*, Vol. 5, No. 5, pp.1093–1102.
- Sangwal, K. (2007) *Additives and Crystallization Processes – From Fundamentals to Applications*, John Wiley and Sons Ltd. England.

- Sanjuan, B. and Girard, J.P. (1996) *Review of Kinetic Data on Carbonate Mineral Precipitation*, BRGM Report R39062, 91pp.
- Santos, L.F., Santos, A.L.A. and Rocha, S.D.F. (2017) 'Fixação de CO₂ em Efluente Salino de Indústria Petroquímica', *Química Nova*, Vol. 40, No. 7, pp.720–725.
- Shen, Q., Wei, H., Zhou, Y., Huang, Y., Yang, H., Wang, D. and Xu, D. (2006) 'Properties of amorphous calcium carbonate and the template action of vaterite spheres', *Journal of Physical Chemical B*, Vol. 110, No. 7, pp.2994–3000 [online] <https://doi.org/10.1021/jp055063o>.
- Sloevink, V.L. and Jenkins, D. (1980) *Water Chemistry*, University of Michigan, Wiley [online] ISBN-10: 0471051969.
- Song, Y., Qian, F., Gao, Y., Huang, X., Wu, J. and Yu, H. (2015) 'PHREEQC program-based simulation of magnesium phosphates crystallization for phosphorus recovery', *Environmental Earth Science*, Vol. 73, No. 9, pp.5075–5084 [online] <https://doi.org/10.1007/s12665-015-4340-8>.
- Subramani, A., Cryer, E., Liu, L., Lehman, S., Ning, R.Y. and Jacangelo, J.G. (2012) 'Impact of intermediate concentrate softening on feed water recovery of reverse osmosis process during treatment of mining contaminated groundwater', *Separation and Purification Technology*, Vol. 88, pp.138–145 [online] <https://doi.org/10.1016/j.seppur.2011.12.010>.
- Sudmalis, M. and Sheikholeslami, R.; (2000) 'Coprecipitation of CaCO₃ and CaSO₄', *The Canadian Journal of Chemical Engineering*, Vol. 78, No. 1, pp.21–31 [online] <https://doi.org/10.1002/cjce.5450780106>.
- Truesdell, A.H. and Jones, B.F. (1974) 'WATEQ, a computer program for calculating chemical equilibria of natural waters', *Journal of Research of The U.S. Geological Survey*, Vol. 2, No. 2, pp.233–274.
- Vermilyea, D.A. (1969) 'The dissolution of Mo and Mg(OH)₂ in aqueous solution', *Journal of Electrochemical Society*, Vol. 116, No. 9, pp.1179–1183 [online] <https://doi.org/10.1149/1.2412273>.
- Wang, G., Li, L., Lan, J., Chen, L. and You, J. (2008) 'Biomimetic crystallization of calcium carbonate spherules controlled by hyperbranched polyglycerols', *Journal of Materials Chemistry*, Vol. 18, pp.2789–2797 [online] <https://doi.org/10.1039/B801943F>.
- Wang, T. and Mucci, A. (2012) 'Breakdown of the Ostwald step rule; the precipitation of calcite and dolomite from seawater at 25 degrees and 40 degrees C', *McGill University, Department of Earth and Planetary Sciences Goldschmidt*, Vol. 76, No. 6, p.2514.
- Wiechers, H.N.S., Sturrock, P. and Morais, G.V.R. (1975) 'Calcium carbonate crystallization kinetics', *Water Research*, Vol. 9 No. 9, pp.835–845 [online] [https://doi.org/10.1016/0043-1354\(75\)90143-8](https://doi.org/10.1016/0043-1354(75)90143-8).
- Zaviska, F., Chun, Y., Heran, M. and Zou, L. (2015) 'Using FO as pre-treatment of RO for high scaling potential brackish water: energy and performance optimization', *Journal of Membrane Science*, Vol. 492, pp.430–438 [online] <https://doi.org/10.1016/j.memsci.2015.06.004>.
- Zhou, G.T. and Zheng, Y.F. (2001) 'Chemical Synthesis of CaCO₃ minerals at low temperatures and implication for mechanism of polymorphic transition', *Journal of Neues Jahrbuch für Mineral Abhandlungen*, Vol. 176, pp.323–343, ESP154017603004.

Supporting information

A The variation of the TDS with increasing alkaline reagent concentration

Figure A.1 Total dissolved solids (TDS) as a function of alkaline reagent/solution ratio

